Canadian Nuclear Society
Waste Management, Decommissioning and Environmental Restoration
for Canada's Nuclear Activities: Current Practices and Future Needs
Ottawa, Ontario Canada May 8-11, 2005

LONG-TERM REGIONAL AND SUB-REGIONAL SCALE GROUNDWATER FLOW WITHIN AN IRREGULARLY FRACTURED CANADIAN SHIELD SETTING

J. F. Sykes[1], E. A. Sudicky[2], S. D. Normani[1], R. G. McLaren[2], M. R. Jensen[3]

[1] Department of Civil Engineering, University of Waterloo, Waterloo, Ontario, Canada N2L 3G1
[2] Department of Earth Sciences, University of Waterloo, Waterloo, Ontario, Canada N2L 3G1
[3] Nuclear Waste Management Division, Ontario Power Generation (H16E22), 700 University Avenue, Toronto, Ontario, Canada M5G 1X6
sykesj@uwaterloo.ca

ABSTRACT

As part of Ontario Power Generation's Deep Geologic Repository Technology Program (DGRTP), activities have been undertaken to further the understanding of groundwater flow system evolution and dynamics within a Canadian Shield setting. This paper describes a numerical case study in which the evolution and nature of groundwater flow, as relevant to the siting and safety of a hypothetical Deep Geologic Repository (DGR) for used nuclear fuel, is explored within representative regional (≈5734 km^2) and sub-regional (≈83 km^2) Shield watersheds. The modelling strategy adopted a GIS framework that included a digital elevation model and surface hydrologic features such as rivers, lakes and wetlands. Model boundary conditions were extracted through GIS automation such that the 3-dimensional characteristics of surface relief, surface water features, in addition to, pore fluid salinities and spatially variable permeability fields could be explicitly incorporated. Further flow system detail has been incorporated in sub-regional simulations with the inclusion of an irregular curve-planar Fracture Network Model traceable to site-specific geologic attributes. Interim modelling results reveal that deep-seated regional flow systems do evolve with groundwater divides within the shallow (<300 m) flow system defined by local scale topography, in particular, major rivers and their tributaries. Within the realizations considered groundwater flow at depths of ≈700 m or more was determined to be essentially stagnant and likely diffusion dominated. The role of fracture zone interconnectivity, depth dependent salinity and spatially variable permeability distributions on flow system response to past glacial events is examined. In demonstrating a case for groundwater flow system stability it is evident that predictive modelling approaches that cannot preserve the 3-dimensional complexity of the watershed-scale groundwater flow system may lead to conclusions that are implausible.

1. INTRODUCTION

As part of the Deep Geologic Repository Technology Program, geoscience work activities are being conducted to advance the understanding of groundwater flow and groundwater flow system evolution in Canadian Shield settings at time and space scales relevant to the safety of a deep geologic repository for used nuclear fuel. A key aspect in this work relates to groundwater flow system behaviour and dynamics at regional and local scales. At these scales, assumed flow system

dimensionality, site specific spatial distribution of physical and chemical properties coupled with transient boundary conditions occurring as a result of long-term climate change may markedly affect concepts of flow system stability as related to groundwater flow paths, hydraulic gradients, velocity fields and residence times. The work also illustrates numerical methods and modelling approaches capable of aiding site characterization in the iterative and multi-disciplinary derivation of a descriptive conceptual geosphere site model(s). An important component of this work is associated with developing methods to improve field data traceability within numerical simulations of heterogeneous and anisotropic flow domains, particularly those influenced by irregular fracture network interconnectivity. This approach is intent on providing a systematic framework with which to assemble complex spatial and temporal geoscientific data sets and conduct quantitative flow system uncertainty analyses.

As part of the analysis a descriptive conceptual model is derived based on field data gathered at the Atomic Energy of Canada Limited (AECL) Whiteshell Research Area (WRA), and information available from international geoscience radioactive waste management programs. The primary goal of the analyses is the prediction and illustration of the sensitivity of groundwater flow pathways and residence times to assumed flow domain boundary conditions and parameters. Of particular interest is the role of topographic and density (salinity) gradients at regional and repository scales on groundwater flow paths. In this study, ArcView Geographic Information System (GIS) is used to facilitate data and model output management and visualization. For the sub-regional scale analyses, the approach includes the explicit inclusion of a site-specific, field constrained Fracture Network Model (FNM). These simulations have provided a reasoned basis to examine and contrast concepts of regional and sub-regional scale groundwater flow system evolution. This approach, consistent with that which could be applied during the initial stages of an iterative site investigation, provides a means to explore and communicate amongst a site characterization team the validity of an interim multi-disciplinary descriptive conceptual geosphere model(s) (i.e. hypothesis testing). In so doing this methodology is intent on enhancing the confidence in geosphere realizations and predictive simulations that underpin safety analyses.

An integrated approach to groundwater flow system modelling was implemented using the dual continuum models FRAC3DVS and SWIFT III. A series of results from 3-dimensional numerical analyses at the regional and sub-regional scale of a characteristic Canadian Shield flow domain is presented. The SWIFT III model is based on the finite-difference method and is fully transient with steady-state options. It fully couples the equations for flow, heat and brine transport via fluid density, fluid viscosity and porosity. The model is applicable to saturated porous and fractured media with a dual porosity formulation being used for the latter. Verification and validation of the well-documented code is provided in Ward *et al*. (1984). FRAC3DVS (Therrien *et al*, 2001) is a numerical algorithm for the solution of three-dimensional variably-saturated groundwater flow and solute transport in discretely-fractured porous media. The model includes a dual-porosity formulation, in which discrete fractures are idealized two-dimensional parallel plates. Versions of the model couple fluid flow with brine transport through the fluid density that is dependant on both pressure and brine concentration. In this paper, both SWIFT III and FRAC3DVS have been used to simulate regional-scale groundwater flow coupled with brine transport; the graphics presented here for the regional scale work are based on the SWIFT III results.

2. DATA BASE FOR REGIONAL SCALE MODELING

The analyses presented in this paper are based on three-dimensional groundwater flow in a hypothetical watershed; however, the properties of the watershed and rock domain are representative of the characteristics of typical crystalline rock systems in the Canadian Shield. The selected watershed has an area of 5734 km^2 and extends 102 km in the east-to-west direction and 94 km in the north-to-south direction. The bedrock geology for the watershed was obtained from a 1:1,000,000 Ontario Geological Survey map. The predominant rock type within the watershed is massive to foliated granodiorite to granite. Smaller areas of potassium feldspar megacrystic units and foliated to massive tonalite to granodiorite, respectively, are also present. The surficial geology of the watershed is predominantly exposed granite with small till covered areas. The Digital Elevation Model (DEM) for the watershed, shown in Figure 1, was developed using a 1:250,000 Natural Resources Canada map.

The surface water features for the watershed are detailed in Figure 2. The vector features obtained from 1:50,000 Natural Resources Canada maps using digital cartography include 505 km^2 of wetlands, 460 km^2 of lakes and 2830 km of rivers. The boundary for the watershed is a surface water divide that was determined using ArcView with the water feature map, the digital elevation contours and the DEM. The watershed contains two sub-basins identified in this study by River A on the north and River B on the south. The two rivers meet near the western boundary of the watershed.

The spatial domain for the watershed was discretized to a depth of 1.5 km using 1,534,080 3-dimensional finite difference grid blocks in 10 layers. The columns and rows were uniformly spaced on a 250 m by 250 m grid that resulted in 408 grid blocks in the east-to-west direction and 376 grid blocks in the north-to-south direction. The vertical discretization is summarized in Table 1. The elevation of the top of the domain was determined using a Visual Basic preprocessor, ArcView and the elevation of the DEM at the location of each grid block center. The bottom elevations of layers 1 to 5 vary to conform to the elevation of the ground surface. The bottom elevation of layer 6 was set to 200 m below sea level throughout the domain. The bottoms of layers 7 to 10 were also assigned constant elevations.

As shown in Figure 2, each surface grid block (layer 1) was characterized using ArcView as being inactive, active, wetland, lake or river. A Type II boundary condition representing recharge was used for the active grid blocks while Type I prescribed heads, equal to the surface elevation, were used for the remaining surface grid blocks. Zero flux boundary conditions were used for the side and bottom boundaries of the spatial domain.

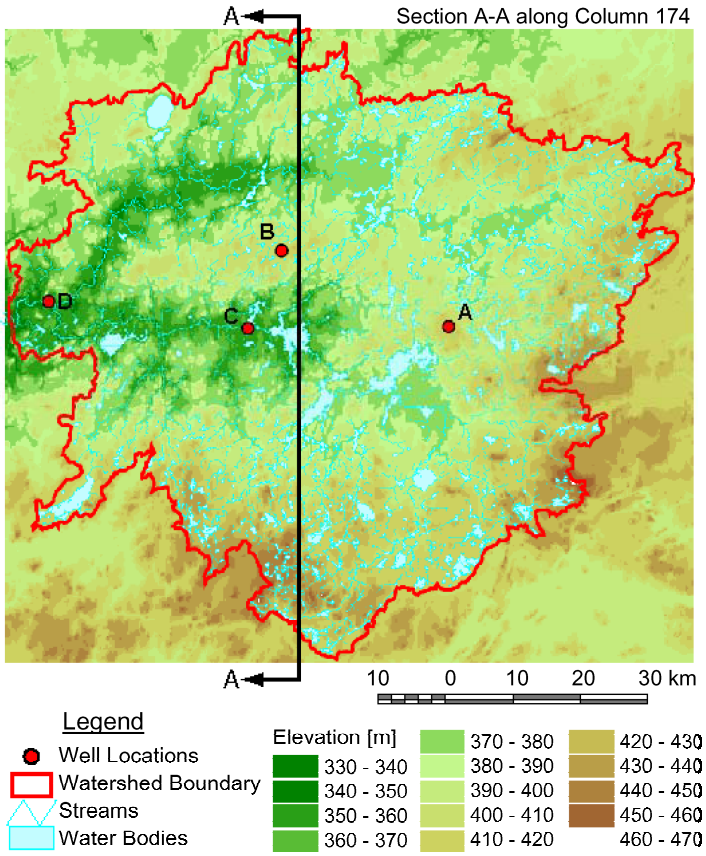

Figure 1: Digital Elevation Model showing location of cross-section and simulation observation wells.

Table 1: Model discretization and hydraulic conductivities

Layer	Depth (m)	Hydraulic Conductivity (m/s)		
		Case 1	Case 2	Case 3
1	10	6.7×10^{-8}	6.7×10^{-8}	6.7×10^{-8}
2	30	6.7×10^{-9}	6.7×10^{-9}	6.7×10^{-9}
3	70	6.7×10^{-9}	6.7×10^{-9}	6.7×10^{-9}
4	150	3.0×10^{-10}	3.0×10^{-10}	3.0×10^{-10}
5	300	4.0×10^{-11}	4.0×10^{-11}	4.0×10^{-11}
6	500	2.1×10^{-12}	2.1×10^{-12}	2.2×10^{-11}
7	700	2.2×10^{-13}	2.2×10^{-13}	2.2×10^{-11}
8	900	9.1×10^{-15}	2.2×10^{-13}	2.2×10^{-11}
9	1100	6.7×10^{-15}	2.2×10^{-13}	2.2×10^{-11}
10	1500	6.7×10^{-15}	2.2×10^{-13}	2.2×10^{-11}

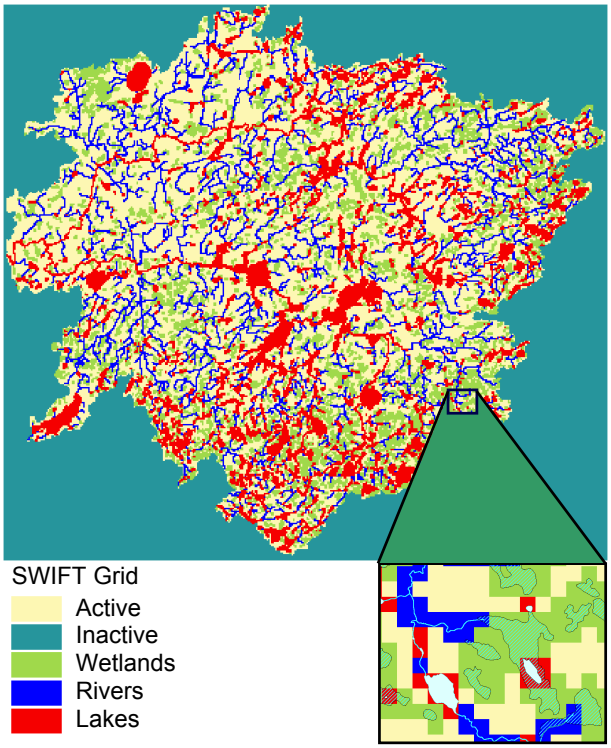

Figure 2: Finite difference grid and water features.

In the modelling presented here, it was assumed that the rock mass is exposed at surface. Two different conceptual models of the change in horizontal hydraulic conductivity with depth were investigated. The Case 1 permeability distribution (refer to Table 1) is derived from depth dependent data given in Stevenson *et al*. (1996) while Case 2 (the base case) and Case 3 investigated groundwater flow in more permeable crystalline rock settings. The lower permeability Case 1 data are presented solely for reference. At the WRA, moderately fractured rock (MFR) is more prevalent to a depth of ≈300 m with the predominant orientation of the fractures reported as vertical. To reflect the presence of MFR, the hydraulic conductivity for model layers 1 to 5 of this study were assumed to be anisotropic with the vertical hydraulic conductivity being arbitrarily assigned a value 10 times greater than the horizontal value. The rock mass represented by model layers 6 to 10 was assumed to be isotropic. A constant porosity of 0.005 was used throughout the domain.

Three initial concentration distributions were assumed for the regional models: freshwater with a density of 1 g/cm^3 throughout the domain; freshwter to a depth of 200 m below sea level (approximately 700 m below ground surface) underlain by either brine with a density of 1.03 g/cm^3 or by brine with a density of 1.1 g/cm^3. The inclusion of a brine layer requires the solution of coupled transient flow and brine transport. For the transient flow system, an initial hydrostatic pressure distribution was calculated for the entire domain using a pressure of 0.0 Pa at an elevation of 450 m and the assumed brine distributions. The specific storage for the rock was calculated using a pore water compressibility of 4.57×10^{-10} Pa^{-1}, a rock compressibility of 0.258×10^{-8} Pa^{-1} and a rock density of 2650 kg/m^3. For the simulation of brine transport, the longitudinal dispersivity was assumed to be 125 m while the molecular diffusion coefficient was assigned a value of 2.5×10^{-12} m^2/s.

3. REGIONAL SCALE ANALYSES

3.1 Base Case Analysis

The calculated steady-state piezometric heads at a depth of approximately 600 m (model layer 7) for the base case analysis and freshwater throughout the domain are shown in Figure 3. A visual comparison of the head distribution with the DEM of Figure 1 supports the conclusion that the heads at a depth of approximately 600 m are a subdued reflection of surface topography.

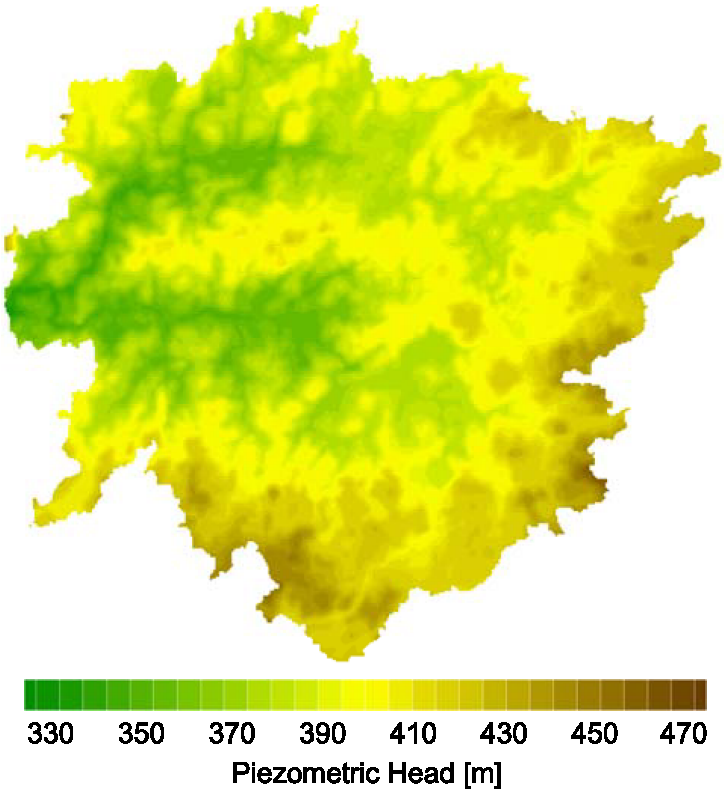

Figure 3: Piezometric head at 600 m for steady-state base case analysis and freshwater.

It has been hypothesized that anomalously elevated piezometric heads measured at depth within the SFR at the WRA are, in part, a result of mechanical and hydraulic loading that occurred during the last glacial cycle. As a result of the extreme low permeability of the SFR, the groundwater flow system responds slowly to pressure changes, and is still in transition. A transient flow analysis was undertaken to test this hypothesis. The 450 m initial head was selected to reflect glacial loading. A comparison of the steady-state results with those at 10,000 years for the transient analysis reveals that the heads at 600 m depth are higher for the transient simulation, with the difference being most readily observed at sub-basin divides. A comparison of the distributions at a depth of approximately 1300 m (model layer 10) indicates that the heads at 10,000 years remain significantly elevated (i.e. above ground surface elevations) as compared to the steady-state case. The higher permeabilities used for the shallower depths allow the heads in those zones to more quickly dissipate and attain steady-state values. The difference in the heads for the two cases is apparent in the piezometric head histograms of Figure 4. Histograms illustrative of head

distributions at the shallower depths are similar for both the steady-state analysis and at 10,000 years for the transient analysis. A comparison of the histograms for the deeper, less permeable rock mass indicates that at 10,000 years, the initial head of 450 m has not been fully dissipated.

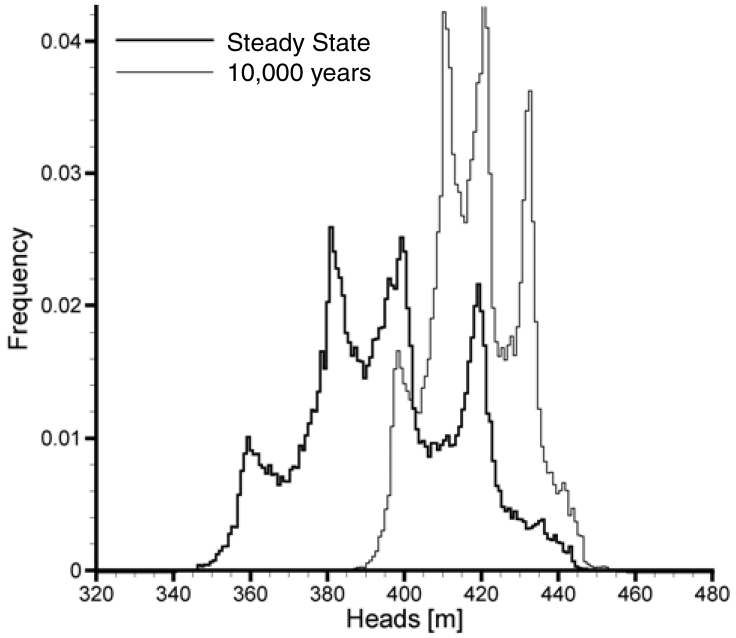

Figure 4: Piezometric head histograms at 1300 m for steady state and transient base case analyses.

Below depths of 600 m, the linear velocities in the rock mass have a low magnitude and are in the diffusive transport range for both the steady-state analysis and at 10,000 years for the transient analysis. Higher velocities in the low permeable rock mass are predicted for the transient case as a where higher vertically upward gradients persist. Near surface the vertical hydraulic gradients spatially appear highest beneath the rivers and lowest at divides between tributaries.

The three-dimensional groundwater flow results for the Base Case parameters (Case 2 in Table 1) do not indicate the presence of regional flow. This conclusion is more readily apparent in the plot of piezometric heads for the north-to-south cross-section shown in Figure 1. The steady-state heads for the cross-section are presented in Figure 5a while the results at 10,000 years for the transient case are presented in Figure 5b. There is no regional flow in the steady-state results; groundwater does not underflow either River A or River B or their main tributaries at any depth in the domain. The transient results clearly reveal the signature of the imposed initial head of 450 m in the lower permeability deeper rock. At 10,000 years, the heads are still elevated at depth as compared to the steady-state values and the flow direction has a dominant upward component.

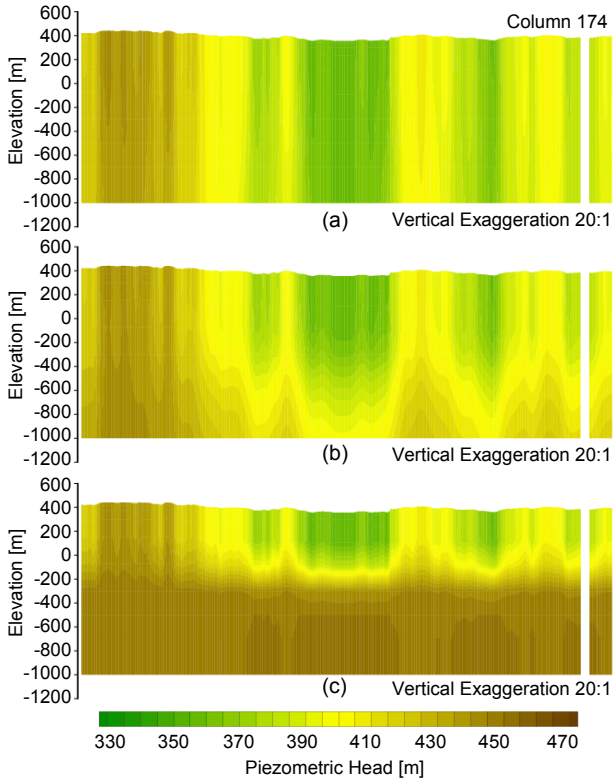

Figure 5: Heads in cross-section for base case parameters (a) steady state, (b) at 10,000 years with freshwater, (c) at 10,000 years with 1.03 g/cm^3 brine.

3.2 Groundwater Flow with Saline Pore Waters In The Deep Rock

High salinity pore waters have been observed at depth at the WRA and elsewhere in the Canadian Shield. To evaluate the impact of the brines on groundwater flow, this study assumed an initial condition consisting of brines in model layers 7 to 10 and freshwater above. Transient simulations of coupled flow and brine transport were conducted using both the Case 2 and the Case 3 models of permeability versus depth. The standard correlation coefficients for these analyses between the pressure at datum (expressed in terms of equivalent freshwater head) in the model layers and the surface topography were calculated. At 10,000 years there is a high negative correlation between the heads in the model layers with brine and the surface topography for the lower permeability Case 2. In comparison, a high positive correlation was calculated at 10,000 years for the higher permeability Case 3 analyses, and for all cases and parameters at 100,000 years. Therefore, the lower permeability of Case 2 coupled with the higher density brine in the deeper rock results in a system that is still recovering (transient) at 10,000 years.

The impact of brine with a density of 1.03 g/cm^3 on the flow domain at 10,000 years for the Case 2 properties is readily observed in Figure 5c. In comparison to the analyses without brine, shown in Figures 5a and 5b, the effect of brine is to retard the dissipation of the elevated head that was initially imposed. For the deeper layers, no regional flow is apparent and the dominant direction of groundwater movement is upward. After 100,000 years, the imposed initial head has been

dissipated and the pattern of groundwater flow is similar throughout the domain to that calculated for the steady-state freshwater case. Transient groundwater flow was also simulated with brine at a density of 1.1 g/cm^3 and the Case 2 parameters. After 100,000 years, the groundwater flow system is near steady-state with the results being similar to those obtained with an initial density of 1.03 g/cm^3 in model layers 7 to 10. The Case 3 permeability distribution with brine at a density of 1.1 g/cm^3 yields similar results. No apparent regional groundwater flow was observed in the results of any of the simulations.

The brine concentrations at 100,000 years for the Case 2 parameters and an initial density of 1.03 g/cm^3 in model layers 7 to 10 are plotted in the cross-section shown in Figure 6. Upward diffusion of the brine is occurring into the shallower rock. The upward brine movement beneath groundwater discharge zones is very apparent. Where groundwater recharge is occurring, the upward migration of the brine has been suppressed. The results reveal that the complex surface topography causes circulation to occur at the shallow local scale; no regional flow system develops. The location of a lake is shown in the cross-section of Figure 6. Groundwater moves from recharge areas through the more permeable shallow rock to the lake margins; the lack of a horizontal gradient beneath the lake results in a diffusive environment and lower brine concentrations under the lake than at the lake margins where transport is by both advection and dispersion.

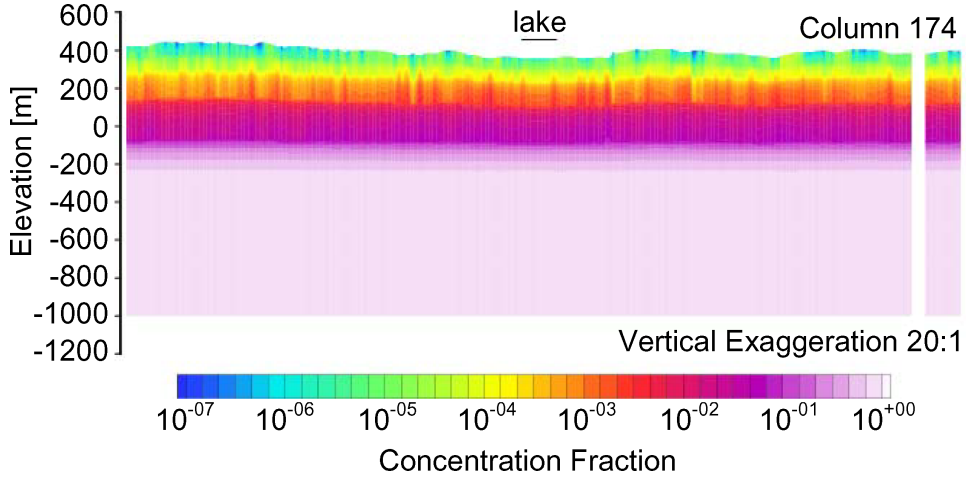

Figure 6: Brine concentrations at 100,000 years for base case parameters and 1.03 g/cm^3 brine.

A plan view of predicted regional-scale salinity distributions at 100,000 years is shown at a depth of 110 m in Figure 7. The simulations are based on the Case 2 permeability model and brine with a density of 1.03 g/cm^3. The highest concentrations occur beneath the groundwater discharge areas associated with Rivers A and B and their tributaries. Lower concentrations are calculated beneath the recharge areas. The higher concentrations that occur at the lake margins outline the lakes. The complex surface topography results in a transition from zones of recharge to discharge over relatively short distances, thus contributing to the complex concentration distribution. The results suggest that field observations of salinity could be useful in identification of groundwater discharge and recharge areas.

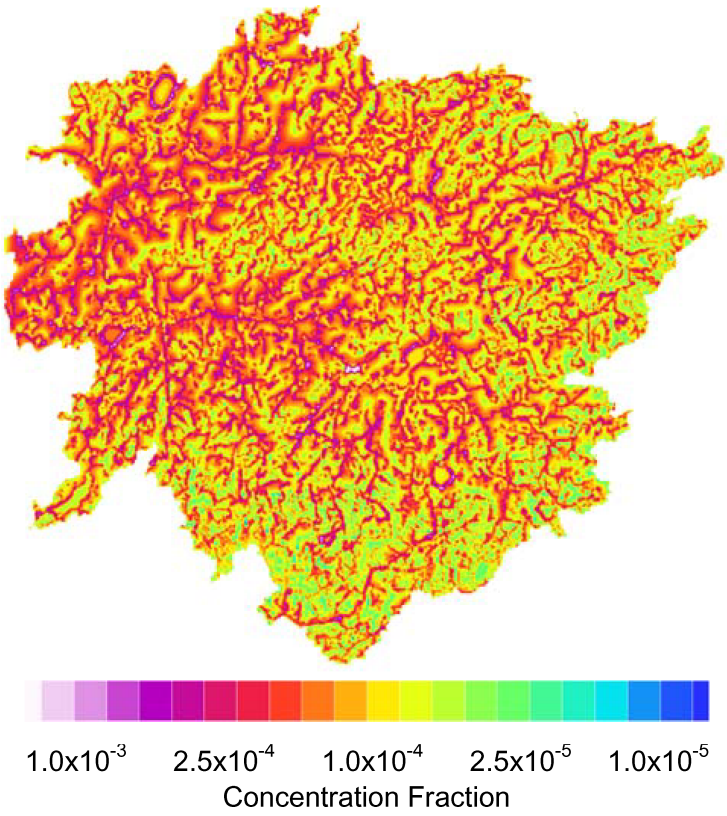

Figure 7: Brine concentrations at 110 m depth at 100,000 years for base case parameters and 1.03 g/cm^3 brine.

3.3 Residual Pressure Dissipation due to Glaciation

With time, the anomalously elevated pressures observed in the SFR at the WRA will dissipate, with the rate being a function of the permeability and storage coefficient of the SFR. The rate of dissipation is also a function of the location and geometry of the permeable rock, as may occur in fracture zones, which bound the SFR. The sensitivity of pressure dissipation to SFR permeability and brine concentrations is investigated; the dissipation of the elevated SFR pressure at permeable fracture zones (FZ) will be considered in future work.

Figure 8 presents the change in pressure with log time in each of the 10 model layers at location D as shown in Figure 1. The pressures are at the elevation of the grid block centers with the lowest pressures in each graph corresponding to the values calculated for layer 1 using the Case 2 parameters and the highest pressures corresponding to those for layer 10. The results show that in the high-permeability shallow layers, the pressures reach equilibrium values very quickly. In comparison, it takes more than 70,000 years for the pressures at a 1300 m depth to reach steady-state. The rate of pressure change is not strongly influenced by the pore water salinity but is dependent on the permeability of the rock. The pressures for the higher permeability Case 3 parameters reach equilibrium levels at all depths in less than 1,000 years. The presence of higher permeability fracture zones at depth will permit a more rapid release in the pressures than the rates calculated without such zones; therefore, the calculated times to steady-state are likely over

estimated. The results support the argument that the permeabilities of Case 2 are more representative of the existence of large domains of SFR than are those for Case 3.

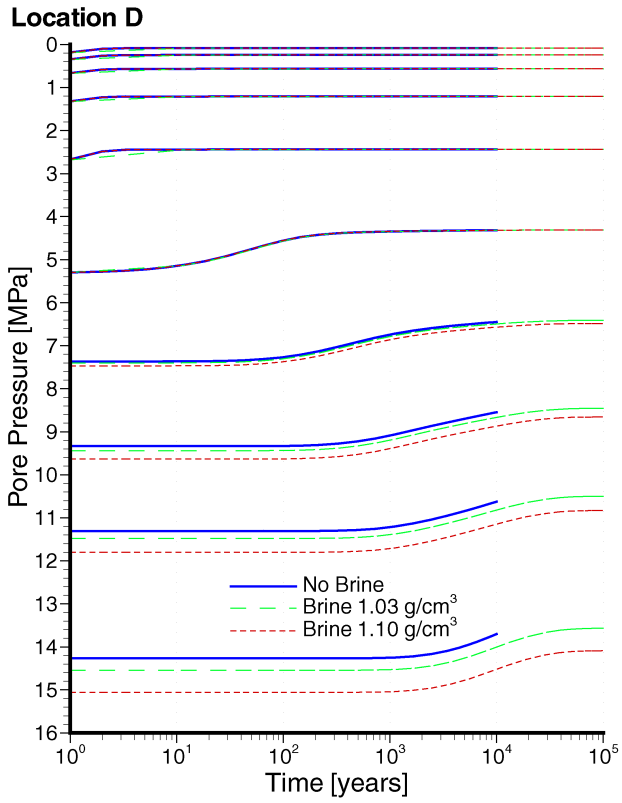

Figure 8: Pressure dissipation with time for each model layer at location D.

4. SUB-REGIONAL STUDY

The hypothetical sub-regional model domain was chosen from several candidate sites within the regional watershed (Figure 9). The hypothetical regional model domain contains two major rivers, a northern and a southern, each draining their respective portion of the larger watershed. Criteria such as the range in topographic relief, as well as, the areal extent, shape, and location of boundary conditions (rivers, lakes, and wetlands) were considered. The chosen domain has an area of approximately 83 km^2, an easting extent of 10.8 km and a northing extent of 12 km as shown in Figure 10. As can be seen in Figure 9, the northern topographic divide of the modelled area is coincident with the watershed divide between the northern and southern rivers.

The FRAC3DVS model was applied to the hypothetical sub-regional site. Various GIS data sources were used to facilitate the development of the sub-regional model:

- Digital Elevation Model (DEM) with a planimetric resolution of 3 arc seconds and a vertical resolution of 1.0 m;
- Digital NTS (National Topographic Service) maps at a scale of 1:50,000 to represent contours, lakes, rivers, wetlands, dams, and other features found on the NTS maps;
- Aerial photography at a scale of 1:60,000 from the National Air Photo Library (NAPL)

The aerial photography was digitized, orthorectified, and mosaiced to the Digital NTS GIS files, as shown in Figure 10.

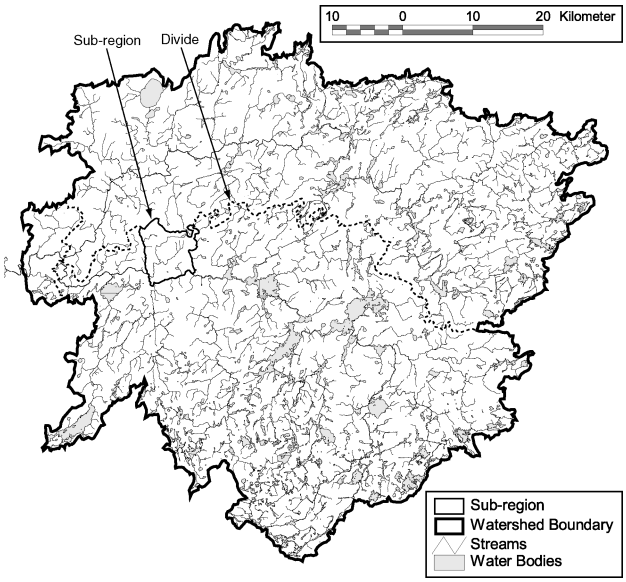

Figure 9: Location of sub-regional model within regional domain.

4.1 Conceptual Descriptive Model Development

Surface water features such as wetlands, lakes and rivers are defined as Dirichlet (Type I) boundary conditions. A Digital Elevation Model (DEM) was used to establish the elevation of these water features, and consequently the top layer of the numerical model. A recharge boundary condition (Type II or Neumann) was not used to represent infiltration from precipitation for the top surface of the model, but rather the Dirichlet boundary condition of fixed piezometric head was applied. This application is based on the fact that the water table is typically a subdued representation of surface topography. The northern model boundary was chosen based on a topographic divide, while the eastern, southern, and western model boundaries were chosen coincident with rivers. An implied assumption, consistent with regional scale simulations, was that such rivers create flow divides beneath which groundwater cannot flow.

The three-dimensional sub-regional domain is discretized into 610,320 nodes, and 568,442 brick elements. The grid is orthogonal with each matrix element having the same planimetric dimensions of 50 m by 50 m. The model is vertically discretized into 19 layers; each layer containing the same number of elements. Vertical thicknesses of layers are presented in Table 2.

Table 2. Assigned sub-regional model properties by layer

Layer	Thickness [m]	Bottom Elev [m]	Hydraulic Conductivity [m/s]		
			Case 1	Case 2	Case 3
19	10	Var.	7.0E-08	7.0E-07	7.0E-07
18	20	Var.	7.0E-09	7.0E-08	7.0E-08
17	40	Var.	7.0E-09	7.0E-08	7.0E-08
16	80	Var.	6.0E-11	8.0E-10	5.0E-09
15	100	Var.	4.0E-12	7.0E-11	1.0E-09
14	100	0	4.0E-12	7.0E-11	1.0E-09
13	100	-100	1.0E-12	3.0E-11	5.0E-10
12	100	-200	1.0E-12	3.0E-11	5.0E-10
11	75	-275	8.0E-13	7.0E-12	5.0E-11
10	50	-325	8.0E-13	7.0E-12	5.0E-11
9	50	-375	8.0E-13	7.0E-12	5.0E-11
8	50	-425	2.0E-13	1.0E-12	1.0E-11
7	50	-475	2.0E-13	1.0E-12	1.0E-11
6	50	-525	2.0E-13	1.0E-12	1.0E-11
5	75	-600	2.0E-13	1.0E-12	1.0E-11
4	100	-700	2.0E-13	1.0E-12	1.0E-11
3	150	-850	2.0E-13	1.0E-12	1.0E-11
2	200	-1050	2.0E-13	1.0E-12	1.0E-11
1	200	-1250	2.0E-13	1.0E-12	1.0E-11

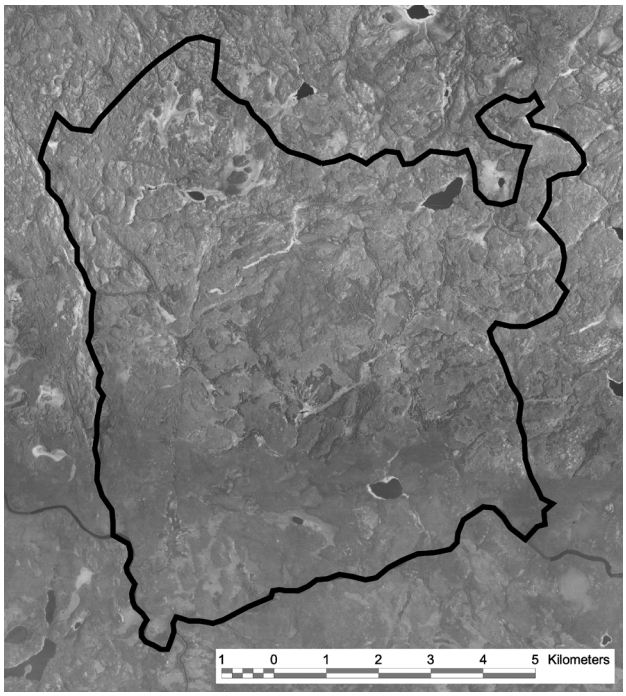

Figure 10: Aerial photograph and modelling boundary for sub-regional model.

The aerial photography served as a basis for developing the various fracture features. A surface lineament analysis was conducted by Srivastava (2002) to define the major fracture features. These fracture features are primarily coincident with surface drainage features that exhibit linearity. Additional surface lineaments were created to account for the extension of existing major lineaments, and to preserve site-specific fracture density in areas where overburden cover would have obscured the surface lineaments or where the aerial photograph had weak contrast, such as the southern third of the image (Figure 10). The resulting surface fracture features are shown in Figure 11.

The surface traces are then propagated to depth until one of the following conditions are met:

- the fracture's down-dip width reaches the prescribed length to width ratio;
- the fracture truncates against an existing fracture; or
- the fracture reaches the edge or bottom of the modelled domain.

These rule based conditions, described in Srivastava (2002), yield FNM surface trace realizations that possess geomechanically plausible fracture behaviour.

Horizontal fracture intersections at ground surface and at a depth of 1000 m are shown in Figures 11 and 12, respectively. As can be seen, fracture density decreases with increasing depth; minor fracture features are shallower than the major fracture features. The resulting discrete fracture network contains a high degree of realism that honours many geological, statistical, and geomechanical constraints (Srivastava, 2002). A three-dimensional view of the discrete-fracture network is shown in Figure 13.

The geometry of individual curve-planar fracture surfaces in the discrete fracture model is described by an interconnected network of triangular facets as depicted in Figure 14. This approach can be used to represent intersecting fracture sets, fractures of virtually any shape or orientation, and to assign spatially variable fracture properties. FRAC3DVS is capable of using tetrahedral elements, but the generation of a 3-dimensional mesh to accommodate the complex geometries and orientations of the 548 discrete fractures was not possible due to the lack of a suitable and robust mesh generator. Because an orthogonal brick finite element mesh was used, software was developed to create an orthogonal fracture that best represents each discrete fracture. The resulting orthogonal fracture representation is shown in Figure 15. The stepped nature of the orthogonal fracture is shown to accommodate both the dip and orientation of the original discrete fracture.

4.2 Model Properties

The FRAC3DVS sub-regional model is comprised of 19 layers. The porosity throughout the modelling domain is assumed to be 0.002. Table 2 lists the layer thickness, the bottom elevation, and the hydraulic conductivity for the three cases. The three cases represent different hydraulic conductivities for the deeper rock. Case 1 represents approx. the 10^{-13} m/s hydraulic conductivity that was used in the EIS study, while Case 3 represents approx. the 10^{-11} m/s hydraulic conductivity that was used in the SCS (Stanchell *et al.*, 1996). Case 2 represents an intermediate hydraulic conductivity of 10^{-12} m/s for the deeper rock, midway between Case 1 and Case 3. The hydraulic conductivities listed in Table 1 are isotropic with respect to the three principal axes for all layers

and all cases. Fracture properties are uniform with a hydraulic conductivity of 10^{-6} m/s for the present study.

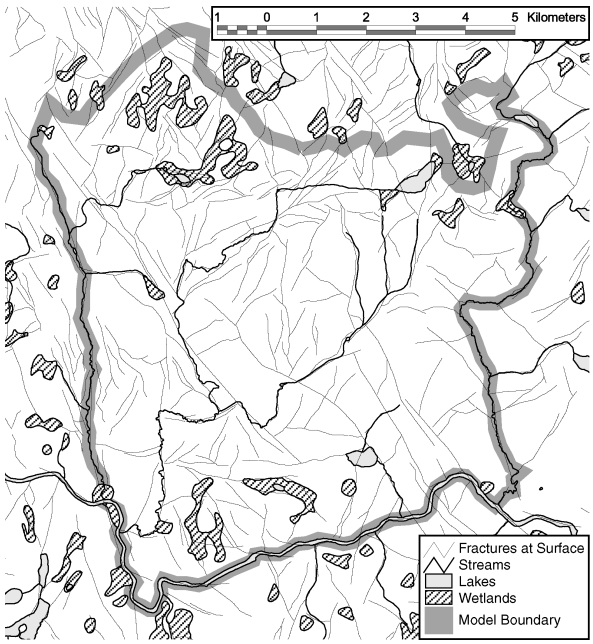

Figure 11: Sub-regional model domain with water features and fractures that intersect ground surface.

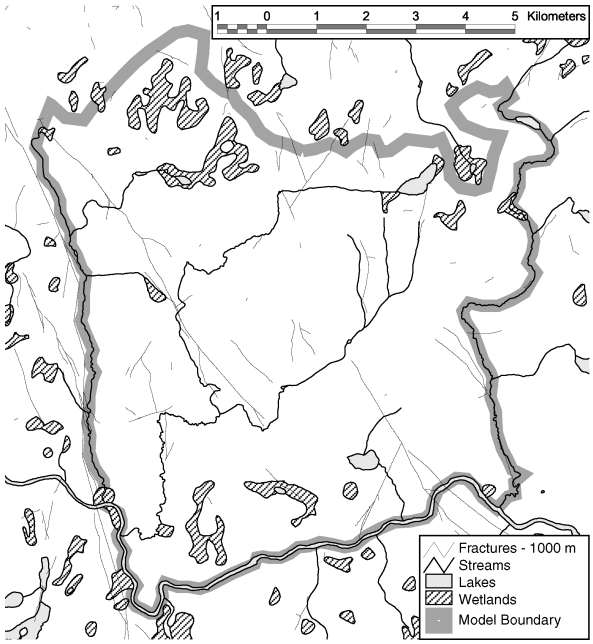

Figure 12: Sub-regional modelling domain with water features and fractures at 1,000 metres depth.

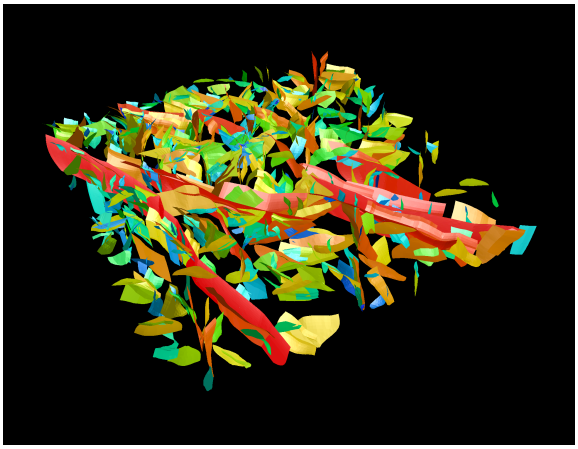

Figure 13: 3-D view of the discrete-fracture network.

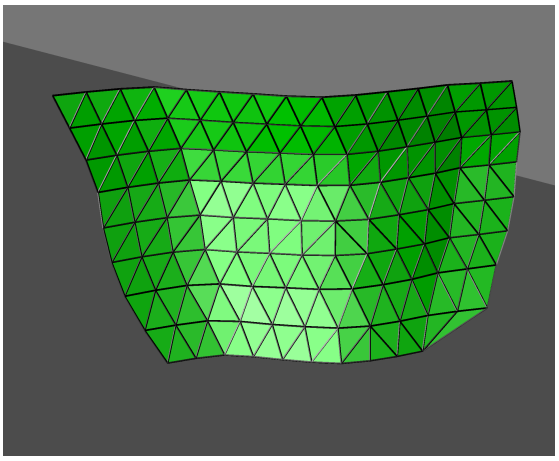

Figure 14: A single triangulated fracture.

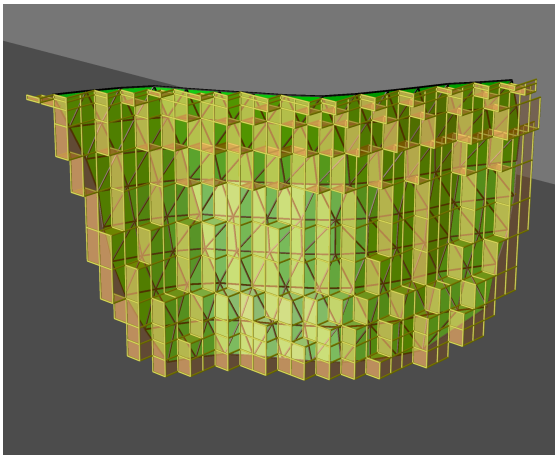

Figure 15: Orthogonal fracture representation of the single triangulated fracture seen in background.

Layers 1 through 14 inclusive have a constant thickness, while Layers 15 through 19 have a variable thickness which depends on the elevation of the ground surface. The thicknesses noted for Layers 15 through 19 add up to a total thickness of 350 m. This base thickness is linearly scaled to account for the variation in the elevation of the ground surface. The thickness of each layer is scaled accordingly.

4.3 Results

As shown in Table 2, three different simulations were performed based on the hydraulic conductivity of the deep rock. Darcy flux magnitudes at the repository level (approximately 500 m depth), and 10,000 year and 1,000,000 year particle tracks are shown in Figure 16 for Case 2.

In Figure 16a, the higher Darcy fluxes are clearly in the fractures (compare to Figure 11). Darcy fluxes in the rock mass matrix are on the order of microns per year and can be considered essentially stagnant; as such, diffusion may represent the dominant transport mechanism. A hypothetical 2.25 km^2 repository footprint is indicated in Figure 16a by the black square drawn in the bottom third of the sub-regional domain. As expected, advective particle tracking from the repository (see Figures 16b and 16c), illustrates that the primary pathway for average water particle migration is via the more permeable pathways, namely fractures. Average water particles must migrate toward and enter fractures before they are able to reach discharge boundaries.

5. SUMMARY AND CONCLUSIONS

An essential requirement for the analysis of regional-scale groundwater flow in variably fractured crystalline rock settings typical of the Canadian Shield is the preservation and accurate description of complex 3-dimensional surface topography, sub-surface permeability distributions, groundwater salinity and surface water drainage networks. This complexity coupled with rock mass permeabilities that decrease significantly with depth results in a groundwater system where shallow flow dominates the overall water balance and advective flow paths at the local scale remain shallow. The flow that occurs in the deeper rock, for example at depths greater than 700 m, represents a very small fraction of the total water budget in the watershed. Further, the analyses presented indicate that the direction of the very low flow in this deeper rock is not regional but rather is influenced by the local-scale surface topography. Where surface water divides occur, coincident groundwater divides also occur. For the hypothetical watershed investigated in this paper, groundwater was not predicted to underflow the major rivers and their tributaries.

Field evidence indicates that the sparsely fractured rock in the Canadian Shield may contain extremely saline pore waters at pressures that may be higher than can be explained by surface topography alone. Transient groundwater models that fully couple flow and brine transport are required to analyze both the impact of the salinity on the groundwater flow system and the dissipation of the elevated pressures for these evolving systems. Steady-state models cannot be used to represent the flow and transport processes that are occurring. The calculation of elevated pressures in deeper rock at 10,000 years from an initial elevated hydrostatic state requires the use of permeability for that rock mass that is less than $2. \times 10^{-11}$ m/s. The impact of the brine and the elevated pressure at depth (below 700 m) is that deep flow is predominantly upward, although estimated Darcy velocities are extremely low.

To include the attributes of a complex surface topography in the watershed conceptual model, this study used ArcView GIS and Visual Basic pre-processors for data management and manipulation. These tools facilitated the development of a discretized model domain with 1,534,080 finite difference grid blocks. Digital input data for the conceptual model included a digital elevation model, a bedrock geology map, a Quaternary geology map and a water features map. Simplifying and possibly conflicting assumptions required of models with reduced physical dimensionality are not necessary because the 3-dimensional nature of topography, surface water features, and the spatial variation of rock permeability have all been natively incorporated within SWIFT-III and FRAC3DVS. Groundwater flow interpretations that are based on simplified models may yield physically implausible results.

A more detailed geosphere study of a hypothetical sub-regional scale Canadian Shield setting has also been performed. The use of realistic topography, delineation of fracture networks that honour many geological, statistical, and geomechanical constraints, and the use of fine discretization grids have improved upon the previous studies of a similar nature. Predicted Darcy fluxes in the rock matrix are on the order of microns per year and can be considered essentially stagnant; as such, diffusion may represent the dominant transport mechanism.

Future realizations of the sub-regional flow system will include simulation of multiple discrete fracture network models, inclusion of variably dense groundwaters, spatially correlated permeability fields within the discrete fracture and matrix continua, and transient analyses to investigate the time history of pore fluid pressure dissipation in discretely fractured crystalline rock within a watershed and for fractures that cross watershed boundaries. Numerical techniques such as sub-timing or sub-gridding can yield significant improvements in model execution time by calculating higher resolution time steps only for those features which are subject to high flow velocities, such as fractures, while the remainder of the computational domain uses a lower resolution time step.

This work is intent on developing a better understanding of flow system evolution at local sub-regional watershed scales, particularly as affected by long-term climate change, and to assess the robustness of numerical prediction given site characterization uncertainty.

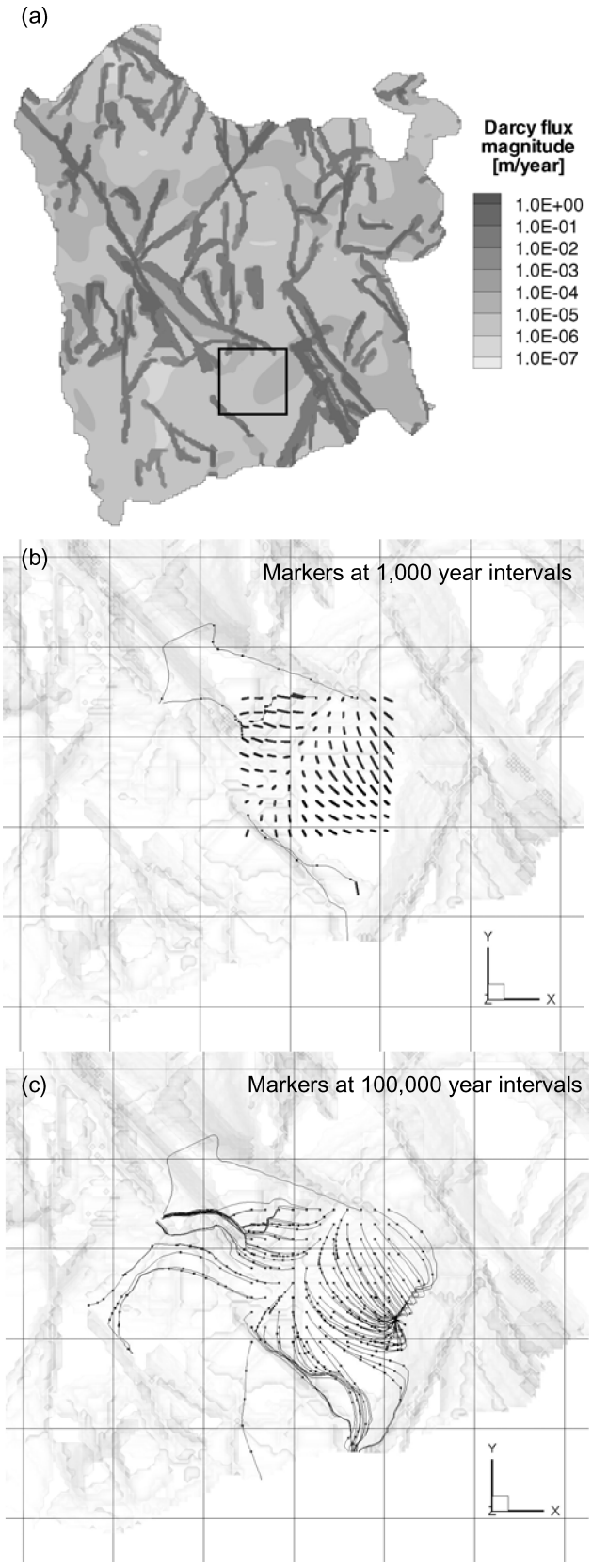

Figure 16: Case 2 results – (a) Darcy flux, (b) 10,000 year particle paths; and (c) 1,000,000 year particle paths.

6. REFERENCES

Normani S.D., J.F. Sykes, E.A. Sudicky and R.G. McLaren, 2003, Modelling Strategy to Assess Long-Term Sub-Regional Scale Groundwater Flow Within an Irregular Discretely Fractured Canadian Shield Setting, Proceedings 4th Joint IAH/CGS Conference September 29-October 1, 2003, Winnipeg, Manitoba, Canada.

Peltier, W.R., 2003, Long-term Climate Change- Glaciation, Ontario Power Generation Nuclear Waste Management Division Report No. 06189-REP-01200-10113 R0.
Srivastava, R.M. 2002. The Discrete Fracture Network Model in the Local Scale Flow System for the Third Case Study. Ontario Power Generation, Nuclear Waste Management Division, Report No: 16819-REP-01300-10061-R00. pp. 1-29. December 2002.

Stanchell, F.W., Davison, C.C., Melnyk, T.W., Scheier, N.W., and Chan, T. 1996. The Disposal of Canada's Nuclear Fuel Waste: A Study of Postclosure Safety of In-Room Emplacement of Used CANDU Fuel in Copper Containers in Permeable Plutonic Rock, Volume 3: Geosphere Model. Atomic Energy of Canada Limited, Report AECL-11494-3, COG-95-552-3. pp 1-54. June 1996.

Stevenson, D.R., Brown, A., Davison, C.C., Gascoyne, M., McGregor, R.G., Ophuri, D.U., Scheier, N.W., Stanchell, F., Thorne, G.A. and Tomsons, D.K. 1996. A Revised Conceptual Hydrogeologic Model of a Crystalline Rock Environment, Whiteshell Research Area, Southeastern Manitoba, Canada. Atomic Energy of Canada Limited, Report AECL-11331, COG-95-271. pp 1-29. April, 1996.

Sykes, J.F., S.D. Normani and E.A. Sudicky, 2003, Regional Scale Groundwater Flow in a Canadian Shield Setting, Ontario Power Generation Nuclear Waste Management Division Report No. 06189-REP-01200-10114 R0.

Sykes, J.F, S.D. Normani and E.A. Sudicky and M.R. Jensen, 2003, Modelling Strategy to Assess Long-Term Regional-Scale Groundwater Flow within a Canadian Shield Setting, Proceedings 4th Joint IAH/CGS Conference September 29-October 1, 2003. Winnipeg, Manitoba, Canada.

Therrien, R., Sudicky, E.A., and McLaren, R.G. 2001. FRAC3DVS: An Efficient Simulator for Three-dimensional, Saturated-Unsaturated Groundwater Flow and Density-dependent, Chain-Decay Solute Transport in Porous, Discretely-Fractured Porous, or Dual-porosity Formations. Mathematical Theory and Verification. R. Therrien, E.A. Sudicky, R.G. McLaren – Groundwater Simulations Group. pp. 1-49. November 26, 2001.